Plasma Detachment with Conventional and Lithium Vapor-Box Divertors

R.J. Goldston*, M.L. Reinke+, J.A. Schwartz*, * Princeton Plasma Physics Laboratory +Oak Ridge National Laboratory

Abstract

The ITER design, and future reactor designs, depend on divertor "detachment," whether partial, pronounced or complete, to limit heat flux to plasma-facing components and to limit surface erosion due to sputtering. It would be valuable to have a measure of the difficulty of achieving detachment as a function of machine parameters, such as input power, magnetic field, major radius, etc. Frequently the parallel heat flux, estimated typically as proportional to P_{sep}/R_0 or $P_{sep}B_0/R_0$, is used as a proxy for this difficulty. Here we argue that impurity cooling is dependent on the upstream separatrix density, which itself must be limited by a Greenwald-like scaling. Taking this into account self-consistently, we find that the impurity fraction $c_z \propto P_{sep} \Big/ \left[\langle B_p \rangle (1+\kappa^2)^{3/2} \left(n_{sep}/n_{GW}\right)^2\right]$. The absence of any explicit scaling with machine size is concerning, as P_{sep} must increase greatly from today's experiments to an economic fusion system, while potential increases in the other parameters are limited. This result should be challenged by comparison with measurements on existing experiments. Nonetheless, it suggests that higher magnetic field, stronger shaping, double-null operation, "advanced" divertor configurations, as well as the lithium vapor-box divertor require greater emphasis.

Impurity Cooling

A simple argument, due to Lengyl[1] and used by others[2,3,4], can be employed in an evaluation of the upstream parallel heat flux that can be dissipated by impurities, which we will assume leads to detachment of the plasma from the material surface of the divertor:

$$q_\parallel = \kappa_{e,\parallel}\frac{dT_e}{d\ell}; \qquad \frac{dq_\parallel}{d\ell} = n_e^2 c_z L_z$$
$$\frac{1}{2}\frac{dq_\parallel^2}{d\ell} = n_e^2 T_e^2 F_z \kappa_0 T_e^{1/2} L_z \frac{dT_e}{d\ell} \qquad eq.1$$
$$q_{\parallel,det} = n_{e,sep} T_{e,sep}\sqrt{2\int_{T_{e,det}}^{T_{e,sep}} F_z \kappa_0 T_e^{1/2} L_z \, dT_e}$$

where $q_{||}$ is the parallel electron heat flux and ℓ represents distance along a field line. $\kappa_{||,e}$ is the parallel electron thermal conductivity, and κ_0 is $\kappa_{||,e}$ divided by $T_e^{5/2}$ for the case of $Z = 1$. κ_0 is taken to be 2600 $Wm^{-1}eV^{-7/2}$. $F_z \equiv c_z \kappa_z$ is the ratio of impurity to electron density, $c_z = n_z/n_e$, multiplied by the finite-Z correction[5] to the $Z = 1$ electron thermal conductivity, $\kappa_z \approx \left(0.672 + 0.076 Z_{eff}^{1/2} + 0.252 Z_{eff}\right)^{-1}$. $n_{e,sep}$ and $T_{e,sep}$ are the electron density and temperature at the upstream separatrix. $T_{e,det}$ is an electron temperature at which it is assumed that detachment of the desired quality is achieved. We evaluate the cooling power taking into account finite impurity lifetime in the plasma. The impurity charge-state distribution is evaluated in steady state, assuming a source of neutral atoms that undergo ionization and recombination as well as loss at a rate common to all charge states, $1/\tau_z$. This non-coronal effect on the charge-state distribution has a large impact on the c_z required for detachment.

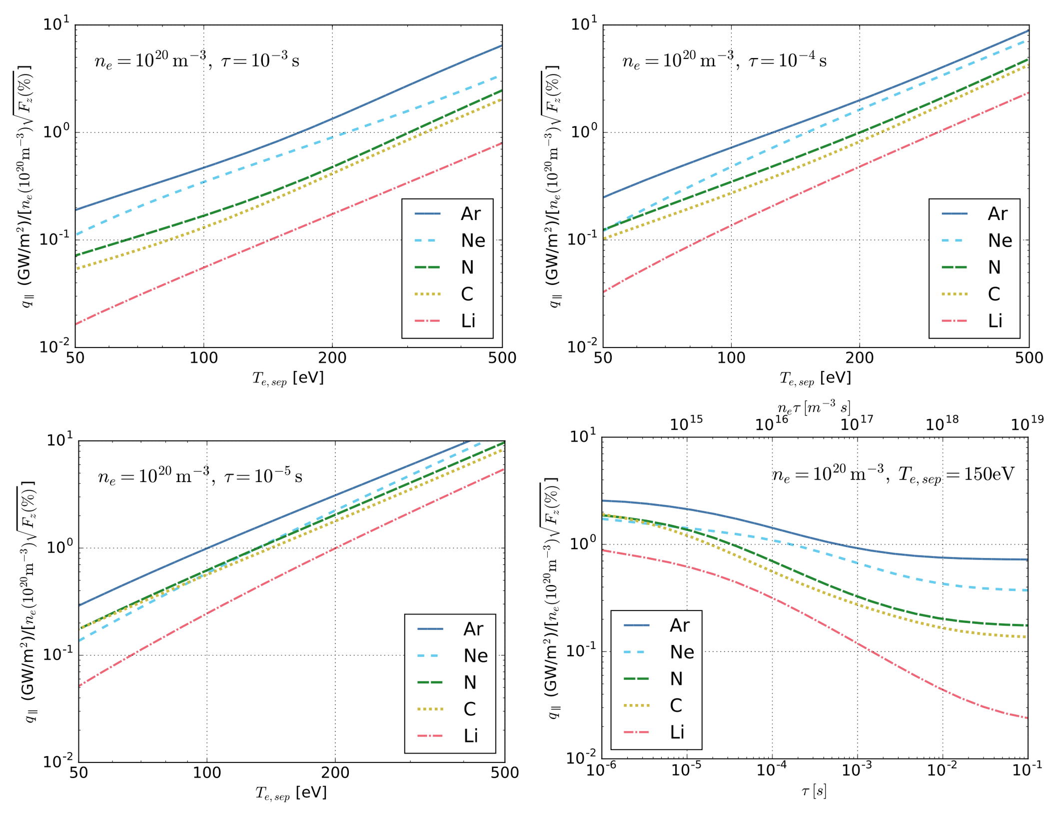

Figure 1: Radiative efficiency vs. impurity, separatrix temperature and $n_e\tau_z$.

Note that the detachable $q_{||}$ scales about as $T_{e,sep}^{3/2}$ over the relevant range of upstream separatrix temperature, T_{sep}, covering existing and future experiments, from about 70 to 300 eV. This implies that the integral in equation 1 scales about as T_{sep}.. It is interesting that the non-coronal effects are strongest on the lower-Z impurities, as shown in figure 1d, making lithium 50% as efficient a radiator as nitrogen at moderate impurity lifetimes. This "finite life-time" collisional-radiative model is crude, as is the assumption that F_z is constant along a field line from the separatrix to the divertor target, but it shoud be indicative of trends and scaling.

The last term required for the R.H.S. of equation 1 is $T_{e,sep}$. If we use Stangeby's two-point model[6] with 100% power loss near the divertor target, we have

$$T_{e,sep} = \left(\frac{7}{2}\frac{q_\parallel \pi q_{cyl} R}{\kappa_z \kappa_0}\right)^{2/7} \qquad eq.2$$

Where the factor $\pi q_{cyl} R$ is chosen to represent an estimate of the divertor connection length in conventional divertor magnetic configurations.

Parallel Heat Flux and Agreement with Other Models and Experiment

Next we evaluate the unmitigated $q_{||}$ that needs to be detached, on the basis of the Heuristic Drift (HD) model[7], which matches the international database for low-gas-puff H-mode data very well both in magnitude and in its specific scalings[8], albeit with an offset (upwards compared with the data) of 1.25. Unlike available empirical fits, the model obeys the constraints of plasma physics. We take the spreading factor S in the Eich fit[9] used in the associated data interpretation at 0.5 λ_q based on measurements[9] and note that this causes the conventional λ_{int} to be 1.79 λ_q. $\lambda_{int} \equiv \int q\, dR \big/ \hat{q}$ and thus relates the peak heat flux to the total.

If we assume, as is conventional, that 2/3 of the plasma transport power crossing the separatrix, P_{sep}, travels to the outer divertor, we have for the peak value of $q_{||}$ at the location where $B = B_0$, the toroidal field at the plasma center, along the outer separatrix field line from the x-point:

$$q_\parallel = \frac{1.25 P_{sep} B_0}{3\pi \cdot 1.79 \langle \lambda_{q,HD} \rangle R_0 \langle B_p \rangle} \qquad eq.3$$

where $\langle B_p \rangle \equiv \mu_0 I_p \Big/ \left[2\pi a \sqrt{(1+\kappa^2)/2}\right]$.

$\langle \lambda_{q,HD} \rangle$ is the poloidally averaged value, given by

$$\langle \lambda_{q,HD} \rangle = 5671 \cdot P_{sep}^{1/8} \frac{(1+\kappa^2)^{5/8} a^{17/8} B_0^{1/4}}{I_p^{9/8} R_0} \left(\frac{2\bar{A}}{1+\bar{Z}}\right)^{7/16} \left(\frac{Z_{eff}+4}{5}\right)^{1/8} \qquad eq.4$$
$$\bar{A} \equiv \sum_i n_i A_i \Big/ \sum_i n_i \qquad \bar{Z} \equiv n_e \Big/ \sum_i n_i$$

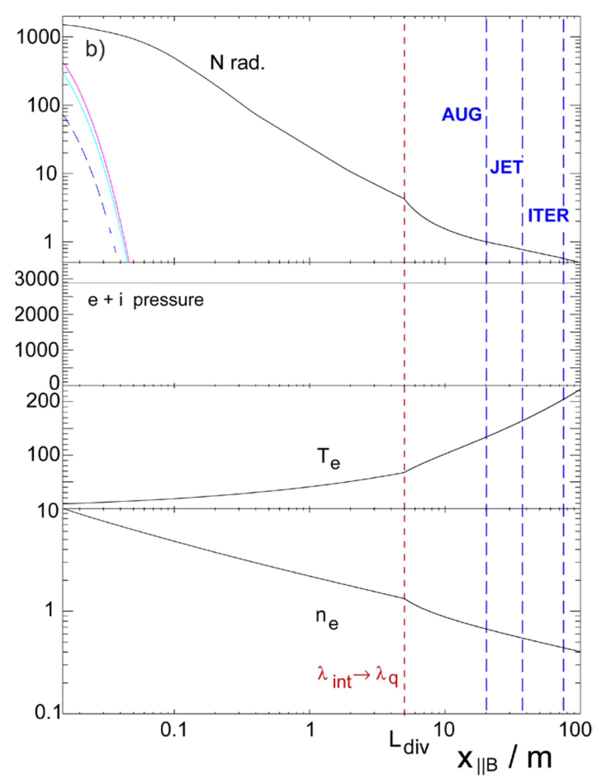

When we compare our simplified model with that of Kallenbach et al.[10], which has been successfully calibrated against experimental data on ASDEX-Upgrade, we find good quantitative agreement.

Note that for fixed magnetic field, consistent with the fixed λ_q assumed in Kallenbach et al.'s figure 4, $n_{e,sep}/n_{GW}$ rises by a factor of about three at fixed $q_{||}$ and $c_N \equiv (n_N/n_e)$ in traversing a factor of five increase in R_0 from ASDEX-Upgrade to EU Demo1, illustrating the limitation of $q_{||}$ as a figure of merit for the difficulty of detachment. At fixed $n_{e,sep}/n_{GW} \sim 1/2$, as in the ASDEX-Upgrade base case, a much greater c_N would be required in EU Demo1.

Figure 4, Kallenbach et al. (2016) Plasma parameters and radiative losses according to the 1D model along the flux tube up to the midplane. The parameters correspond to semi-detached divertor conditions: divertor nitrogen concentration $c_N = 0.04$, $T_{e,tar} = 2.3$ eV, power load of 2.3 MW m^{-2}, $f_{mom} = 0.5$, neutral pressure $p_0 = 4.9$ Pa. The power width λ is reduced from 5 mm to 2 mm at the divertor entrance L_{div}. Dashed vertical lines indicate the midplane for devices of different size. P_{sep} is 10.8 MW for the AUG size ($R = 1.65$ m, $L = 20$ m) and 62 MW for the case with $R = 8.25$ m, $L = 100$ m.

Scaling

The agreement with ASDEX-Upgrade results and modeling above suggests that it could be valuable to consider the scaling of this result from existing to future devices. We will solve for the impurity concentration required as a function of global parameters. We start from equation 1, noting that the term on the RHS scales about as $T_e^{3/2}$. Multiplying both sides by R_0 and normalizing the separatrix density to the Greenwald limit for the bulk plasma, we have:

$$q_\parallel R_0 \propto \left(\frac{q_{cyl} q_\parallel R_0}{\kappa_z}\right)^{3/7} F_z^{1/2} f_{GW,sep} \frac{R_0}{a} \langle B_p \rangle (1+\kappa^2)^{1/2}$$
$$F_z f_{GW,sep}^2 \propto \frac{(q_\parallel R_0)^{8/7}}{\left(\frac{q_{cyl}}{\kappa_z}\right)^{6/7} \left(\frac{R_0}{a}\right)^2 \langle B_p \rangle^2 (1+\kappa^2)} \qquad eq.5$$

Already there is something revealing about this result. $q_{||}$ only appears in the combination $q_{||}R_0$ and no variable with dimension of length appears elsewhere. Since $q_{||}R_0$ scales as $P_{sep}B_0/(\langle B_p \rangle \lambda_{int})$, and our experimental data and the HD theory indicate that λ_{int} itself carries no explicit scaling with machine size, we can see already that there is no explicit size scaling to mitigate the effects of increasing P_{sep} with size, in particular on the requirement for increased impurity concentration.

We proceed to evaluate the scaling of $q_{||}R_0$ from equations 3 and 4. The final term in equation 4 is the result of a less accurate form for κ_z, so we use the form developed here instead.

$$q_\parallel R_0 \propto P_{sep}^{7/8} B_{t,0}^{3/4} \langle B_p \rangle^{1/8} \frac{R_0}{a} (1+\kappa^2)^{-1/16} \left(\frac{\bar{A}}{1+\bar{Z}}\right)^{-7/16} \kappa_z^{1/8} \qquad eq.6$$

Now we have

$$F_z f_{GW,sep}^2 \propto \frac{P_{sep} B_{t,0}^{6/7} \left(\frac{\bar{A}}{1+\bar{Z}}\right)^{-1/2} \kappa_z^{1/7}}{\left(\frac{R_0 q}{a\kappa_z}\right)^{6/7} \langle B_p \rangle^{13/7} (1+\kappa^2)^{15/14}} \qquad eq.7$$

leading to the final result, in which κ_z cancels out:

$$c_z \propto \frac{P_{sep}}{\langle B_p \rangle (1+\kappa^2)^{3/2} f_{GW,sep}^2} \left(\frac{1+\bar{Z}}{\bar{A}}\right)^{1/2} \qquad eq.\ 8$$

For a single impurity, and hydrogenic species with average atomic mass A_H, we find

$$\left(\frac{1+\bar{Z}}{\bar{A}}\right)^{1/2} = \left[\frac{2 - c_z(Z-1)}{A_H(1 - Zc_z) + A_z c_z}\right]^{1/2} \qquad eq.\ 9$$

This is the term that scales the sound speed in a hydrogen plasma for fixed $T_e = T_i$ to an impure and/or deuterium or deuterium-tritium plasma. One could neglect this factor as unproven by experimental results. However recent experiments on JET may have shown its effect in comparing the H-mode density limit for H and D plasmas[11]. For a 50% replacement of deuterons with fully stripped nitrogen ions, it has only an 11% effect, reducing the required c_N. Note, however, that a population of heavy, partially stripped impurities could have a larger effect, as can be evaluated using equation 9.

Discussion

Our result implies increasing difficulty as fusion systems move to separatrix powers an order of magnitude greater than presently employed, while increasing magnetic fields by a factor of ~ 2 – 3, since there may not a be a factor of three headroom above present impurity seeding levels for a fusion power system.

	ASDEX-U	JET	ITER	FNSF (A=4)	EU Demo1
P_{sep}	10.7	14	100	107	150
B_t	2.5	2.5	5.3	7.5	5.7
R_0	1.6	2.9	6.2	4.8	9.0
P_{sep}/R	6.7	4.8	16.1	22.3	16.7
$P_{sep}B_t/R$	16.7	12.1	85.5	167.2	95.0
I_p	1.2	2.5	15	7.9	20
a	0.52	0.90	2.00	1.20	3.00
κ_{95}	1.63	1.73	1.80	2.10	1.70
$\langle B_p \rangle$	0.34	0.39	1.03	0.80	0.96
q*	3.16	2.79	2.42	3.85	2.77
n_{GW}	1.44E+20	9.82E+19	1.19E+20	1.75E+20	7.07E+19
$c_N \propto P_{sep}/(\langle B_p \rangle (1+\kappa^2)^{3/2})$	4.0%	4.1%	10.1%	9.7%	18.6%

Table 1: Some comparisons with recent operating points on existing devices, and future projections. c_N is normalized to the ASDEX-Upgrade case from reference 10. Note that c_N is evaluated in the divertor, so the nitrogen is not fully ionized, and c_N in the core of ASDEX-Upgrade is observed to be significantly lower. P_{sep} is reduced by 40% for the double-null divertor in the Fusion Nuclear Science Facility (FNSF). EU Demo1 employs core radiation to limit P_{sep} to just above the requirement to sustain H-mode confinement.

This work indicates the strong need for new experimental methods to measure c_z in the SOL, and determine if, indeed, the c_z in the SOL required for detachment scales as predicted here. These measurements also need to be compared with more sophisticated models that include plasma transport in evaluating the spatial dependence of c_z, as well as in determining the non-coronal deviation from charge-state balance.

Despite the uncertainties, the present result suggests that there may be considerable advantage to higher magnetic field, even though higher B results in greater $q_{||}$. Strong shaping, which both directly reduces the needed c_z and also allows higher poloidal magnetic field strength at fixed q_{cyl}, reduces c_z further, possibly in conjunction with lower aspect ratio. Future designs should explore options for higher magnetic field, strong shaping including varying aspect ratio, double-null operation, and advanced divertor configurations that may encourage detachment through larger $L_{||}$ and/or reduced B as the divertor target is approached.

The results shown in figure 1 indicate that lithium is only a factor of about 2 less efficient at dissipating $q_{||}$ than nitrogen, for given c_z. In conjunction with Table 1, this suggests that even in a tokamak fusion power system optimized for detachment, the ions in the divertor plasma will need to be largely impurities, whatever their species. Experiments and modeling[12] have shown that very little lithium is transported from the divertor and SOL into the main plasma in current experiments, while higher-Z impurities are often observed in the core at significant concentrations. Furthermore, in the lithium vapor-box concept, lithium vapor is effectively localized in the divertor region through differential pumping via condensation. This should make collapse of the radiating zone to the region within the main plasma near the x-point an unlikely scenario. Thus a divertor plasma dominated by recycling lithium ions and lithium vapor may be a more credible option than one dominated by higher-Z puffed impurities.

Acknowledgments

Authors R.G. and M.R. would like to thank the University of Leiden Lorentz Center "Taming the Flame" workshop for providing the atmosphere in which these ideas could most easily be fleshed out. This work was supported by DOE Contracts Numbers: DE-AC02-09CH11466 and DE-AC05-00OR22725.

[1] L.L. Lengyl, IPP Report 1/191 (1981)
[2] K. Lackner and R. Schneider, Fusion Engineering and Design **22** 107 (1993)
[3] D. Post et al., Phys. Plasmas **2** (2328) 1995
[4] A. Kallenbach et al., Plasma Phys. Control. Fusion **55** 12404 (2013)
[5] S.I. Braginskii, Reviews of Plasma Physics V1, 1965
[6] P. Stangeby, The Plasma Boundary of Magnetic Fusion Devices (2000) Bristol, IOP
[7] R.J. Goldston, Nucl. Fusion **52** 013009 (2012)
[8] R.J. Goldston, J. Nucl. Mat. **463** 397 (2015)
[9] T. Eich et al., Nucl. Fusion **53** 093031 (2013)
[10] A. Kallenbach et al., Plasma Phys. Control. Fusion **58** 045013 (2016)
[11] A. Huber et al., IAEA FEC 2016
[12] F. Scotti, Ph.D. Thesis, T-10 at IAEA FEC 2016